ORIGINAL PAPER

Preparation and Properties of Thermoplastic Starch/Montmorillonite Nanocomposite Using N-(2-Hydroxyethyl)formamide as a New Additive

Hongguang Dai · Peter R. Chang · Fengying Geng · Jiugao Yu · Xiaofei Ma

Abstract N-(2-Hydroxyethyl)formamide (HF) was synthesized efficiently and used as a new additive to prepare thermoplastic starch/montmorillonite nanocomposite (TPS/MMT). Here, HF acted as both plasticizer for TPS and swelling agent for MMT. The hydrogen bond interaction among HF, starch and MMT was proven by Fourier-transform infrared (FT-IR) spectroscopy. By scanning electron microscope (SEM), starch granules were completely disrupted. Atomic force microscopy demonstrated that partially exfoliated TPS/MMT nanocomposite was formed. The crystallinity of corn starch, MMT, HF-plasticized TPS (HTPS) and TPS/MMT nanocomposite was characterized by X-ray diffraction (XRD). Thermal stability of HTPS and TPS/MMT was determined by thermogravimetric analysis (TGA). The water resistance of TPS/MMT nanocomposite increased compared with that of pure HTPS. Tensile strengths of TPS/MMT nanocomposites were higher than those of HTPS, but just the reverse for elongations at break.

Keywords N-(2-Hydroxyethyl)formamide ·
New additive · Thermoplastic starch · Nanocomposites ·
Environmental degradation

H. Dai · F. Geng · J. Yu (✉) · X. Ma
School of Science, Tianjin University, Tianjin 300072,
People's Republic of China
e-mail: tjusmd@yahoo.com.cn

P. R. Chang
Bioproducts and Bioprocesses National Science Program,
Agriculture and Agri-Food Canada, 107 Science Place,
Saskatoon, SK S7N 0X2, Canada

Introduction

The improper disposition of the enormous volume of petroleum-derived plastics in the environment leads to environment pollution and raises the question how to replace them with biodegradable and renewable natural polymers. Currently, much research is concerned with starch, the polysaccharide of granular structure, because it is inexpensive and abundant [1]. The development and production of biodegradable thermoplastic starch (TPS) is important to reduce the total amount of plastic waste. During the thermoplastic process, plasticizers play an indispensable role, because the plasticizers could form the hydrogen bonds with starch, take the place of the strong action between intra- and intermolecular hydrogen bonds in starch, and make starch display the plasticization. In most literature for TPS, polyols as plasticizers usually are used such as glycerol [2], glycol [3], xylitol [4], sorbitol [5], sugars [6]. Amides such as urea [7], formamide [1] and ethylenebisformamide [8] are considered to promote the plasticization of starch too. The type of plasticizer influences the properties of TPS.

The main disadvantages of TPS are its pronounced hydrophilic character, the fast degradation rate and, in some cases, unsatisfactory mechanical properties, particularly in wet environment [9]. However, these features can be significantly improved by blending with montmorillonite (MMT). A few of MMT in nano-scale (below 5 wt%) can dramatically increase the mechanical properties and water resistance of TPS [10]. Research on biodegradable thermoplastic starch/montmorillonite (TPS/MMT) nanocomposites has been a focus in recent years. In order to achieve intercalated or exfoliated TPS/MMT nanocomposite, organo-modified MMT (OMMT) with wider d-spacing is used. However, the low compatibility between hydrophobic

organically modified clay and hydrophilic starch reduce the diffusing of starch molecules into clay galleries and lower the effect of shearing force. But the effect is not obvious [11]. Moreover, the modification of clay is a fussy process in which a great deal of water and organic compound are used, and the nano-MMT granule can re-agglomerate inevitably.

Hydrophobic organically modified clay is favorable to compound with most of synthesized polymers, but it is immiscible with hydrophilic biomacromolecules such as starch. Therefore, it can be concluded that using hydrophilic modified clays could be a promising way to further improve clay exfoliation [11].

Some studies find the plasticizer (water and glycerol) can intercalate into the narrow d-spacing of MMT effectively [11]. Swelling the silicate in glycerol results in the adsorption of some of the plasticizer and an extension of gallery distance reached to around 1.8 nm, which might be further modified during processing. According to Ishida and coworkers [12, 13], the use of a small amount of swelling agent may facilitate intercalation. For example, Bagdi et al. [14] swell silicate in glycerol for 1 day and then homogenize it with the starch powder. Intercalation and partial exfoliation occur during processing.

Traditional plasticizer glycerol could act as swelling agent for MMT. However, the properties of TPS/MMT do not reach what people expect. Here, plasticizer for TPS and swelling agent for MMT are called additives. The type of additives influences the properties of TPS/MMT. In views of the application and development of starch materials, it is very important to prepare a low cost and nontoxic additive, which is used to produce TPS/MMT nanocomposites with desired properties. Some work has been done to research the relationship of plasticizers structure and TPS properties [15]. At present, the type of additive is limited. So In theory, the preparation of new additives is also necessary to study the relationship of additives structure and TPS/MMT properties.

N-(2-Hydroxyethyl)formamide (HF) serves as physiologically harmless humidifier for cosmetics [16] or for the impregnation of tire-cord made from nylon [17]. Many synthetic methods for preparation of HF have been reported. However, some of these methods suffer from drawbacks such as high pressure [18], and use of much methanol as solvent [19] which means more complex process.

In this paper, an efficient and practical method is used to synthesize HF without any solvent. As an additive, HF is used to prepare TPS/MMT nanocomposites. Here, HF acts as plasticizer for TPS and swelling agent for MMT. This work is focused on processing and characterization of TPS/MMT nanocomposites in terms of FT-IR, morphology, XRD, water vapour absorption and mechanical properties.

Experimental

Materials

Corn starch (7.62% moisture) was obtained from the Langfang Starch Company (Langfang, Hebei, China). Glycerol, ethanolamine and ethyl formate (analytical grade) were purchased from Tianjin Chemical Reagent Ltd. (Tianjin, China). Sodium montmorillonite (Na^+-MMT) with a cation exchange capacity (CEC) of 90–100 mmol/100 g as an inorganic host material was supplied by Zhangjiakou Qinghe Chemical Plant (Heber, China).

Methods

Synthesis of N-(2-Hydroxyethyl)formamide

1 mol ethanolamine was charged in a 500 mL flask equipped with a stirrer, a reflux condenser, a dropping funnel and a thermometer. When ethanolamine was cooled to 15 °C in an ice bath, 1 mol ethyl formate was dropped during 45 min. The temperature of the mixture rose to 20 °C due to this exothermic reaction. The reaction mixture was stirred for 1 h at 60 °C by monitoring with thin layer chromatography (TLC). Then the byproduct ethanol evaporated under reduced pressure at 60 °C until ethanol was not distilled from the mixture again. Subsequently the mixture was cooled to 15 °C in an ice bath, followed by addition of 0.05 mol ethyl formate. The reaction mixture was stirred for 0.5 h at 60 °C, and then the byproduct ethanol evaporated under reduced pressure at 60 °C until ethanol was not distilled from the mixture again. The residue was cooled to 15 °C in an ice bath, followed by addition of 0.05 mol ethyl formate. The reaction mixture was stirred for another 0.5 h at 60 °C, heated under reduced pressure at 105 °C until the mass of the liquid was constant. A viscous liquid was obtained. The purity 96% was tested by the column chromatography on neutral aluminum oxide (200–300 mesh) eluted with mixture of dichloromethane and methanol. The yield of HF was 97%. The product was confirmed by IR, ^{1}H NMR, MS. The chemical reaction equation was shown in Fig. 1.

^{1}H NMR spectra were measured on a VARIAN INOVA 500 MHz spectrometer using TMS as internal standard and CD_3SOCD_3 as solvent. The IR spectra were recorded with a BIO-RAD FTS3000 IR spectrometer (KBr). Mass spectra were determined on an LCQ Advantage MAX spectrometer (ESI).

Data for N-(2-Hydroxyethyl)formamide v_{max} (KBr): 3551–3259 (OH and NH), 2947 (–CH_2–), 2887 (–CH_2–), 1661 (C=O) cm^{-1}; ^{1}H NMR (CD_3SOCD_3, δ ppm): 7.983–7.870 (m, 4H, HCONH), 4.717 (t, 1H, J = 5.5 Hz, –OH), 4.693

Fig. 1 Chemical reaction equation of synthesizing *N*-(2-hydroxyethyl)formamide
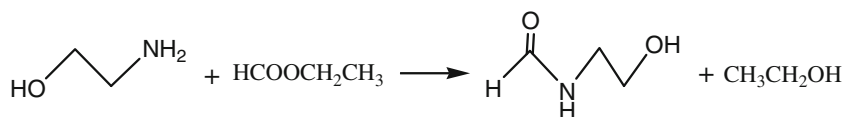
(t, 1H, J = 5.5 Hz, –OH), 3.390 (q, 2H, J = 6.0 Hz, –CH$_2$O–), 3.362–3.326 (m, 2H, –CH$_2$O–), 3.126 (q, 2H, J = 6.0 Hz, –CH$_2$N), 3.084 (q, 2H, J = 6.0 Hz, –CH$_2$N), *m/z* (%): 90 (MH$^+$, 100), 112 (MNa$^+$, 12.3).

Preparation of TPS and TPS/MMT Nanocomposites

HF was blended (3000 rpm, 2 min) with corn starch in the high speed mixer GH-100Y (Beijing Plastic Machinery Factory, Beijing, China), and then stored overnight. The mass ratio of HF to corn starch was 30:100. The mixtures were manually fed into the single-screw plastic extruder SJ-25(s) (screw ratio L/D = 25:1, Beijing Plastic Industry Combine Corporation, Beijing, China) with a screw speed of 15 rpm. The temperature profile along the extruder barrel was 130, 125, 130 and 130 °C (from feed zone to die). The die was a round sheet with holes 3 mm in diameter. The extruded samples were obtained.

TPS/MMT nanocomposites were prepared in two steps processing conditions. In the first step, pristine MMT (PMMT) and HF were stirred at 120 °C for 3 h, the ratio were 2:30, 5:30 and 8:30. A pulp was obtained and named HF-modified MMT (HMMT). The HMMT was blended (3000 rpm, 2 min) with corn starch in the high speed mixer GH-100Y, and then stored overnight. The mass ratio of HF to corn starch was 30:100. The mixtures were manually fed into the single-screw plastic extruder SJ-25(s) with a screw speed of 15 rpm. The temperature profile along the extruder barrel was 130, 125, 130 and 130 °C (from feed zone to die). The die was a round sheet with holes 3 mm in diameter. The extruded samples were obtained.

Morphology

Scanning Electron Microscopy (SEM)

Corn starch, MMT and the fracture surfaces of the HTPS samples were investigated with the scanning electron microscope Phillips XL-3 (FEI Company, Hillsboro, OR, USA), operating at an acceleration voltage of 20 kV.

Starch or MMT powders were suspended in acetone. The suspension drops were drawn on the glass slide, dried for removing the acetone, and then vacuum-coated with gold for SEM. The conditioned HTPS sample was cryo-fractured in liquid nitrogen. The fracture faces were vacuum-coated with gold for SEM.

Atomic Force Microscopy (AFM)

The extruded TPS/MMT strips were pressed to the slices at 10 MPa and 100 °C using a flat sulfuration machine (Beijing Plastic Machinery Factory) and the slices were scanned using AFM. AFM studies were carried out in air at ambient conditions (20 °C, 50% relative humidity (RH)) using a multimode AFM from Digital Instruments, Santa Barbara, CA. Topographic (height) and phase (phase contrast) images were recorded in the TMAFM attached with a Nanoscope IIIa feedback controller, equipped with a Nanoscope Extender Ex-1 module to provide simultaneously height and phase mapping. The scan angle was slightly rotated and scan speed was also carefully varied slowly without disturbing the image quality to ensure the proper morphology detected by AFM tip devoid of any tip-arti-facts. Phase images were captured in tapping mode using etched silicon probe tips (RTESP), with a spring constant in the range of 40 N/m. The cantilever was oscillated at its resonance frequency (ω_0) of ∼280 kHz. All phase images were taken as detected. Effect of Fourier transform filtering was checked with tapping mode height image.

Fourier-Transform Infrared (FT-IR) Spectroscopy

The IR spectra were measured with a BIO-RAD FTS3000 IR Spectrum Scanner (Hercules, CA, USA). The HTPS and TPS/MMT samples were pressured to transparent slices at 10 MPa and 100 °C using the Flat Sulfuration Machine (a compression molder), and measured in reflection mode.

X-Ray Diffraction (XRD)

The extruded HTPS and TPS/MMT strips were pressed to the slices with a flat sulfuration machine (Beijing Plastic Machinery Factory) and the slices were placed in a sample holder for X-ray diffractometry. The corn starch or MMT powders were packed tightly in the sample holder. X-ray diffraction patterns were recorded in the reflection mode at an angular range of 2–30° (2θ) at the ambient temperature by a Rigaku D diffractometer (Japan) operated at the Cu Kα radiation.

Thermogravimetric Analysis (TGA)

HTPS and TPS/MMT were cut into small flakes weighing about 5–10 mg, which were tested in a STA409PC thermal

analysis instrument (NETZSCH company, Germany). The temperature range was from 30 to 500 °C at a heating rate of 10 °C/min under nitrogen flow.

Water Vapour Absorption

Measurement of Water Contents of New HTPS and TPS/MMT Nanocomposites

The bars of samples were cut into small pieces and the pieces weighed immediately. They were then dried in an oven at 105 °C overnight. The original water content (k) of TPS was calculated as follows:

$$k = \frac{w_1 - w_2}{w_1} \times 100\% \qquad (1)$$

Here w_2 was the mass of the dried sample and w_1 was the mass of the sample before drying. The data were averages of 3 specimens.

Measurement of Water Contents of HTPS and TPS/MMT Nanocomposites Stored at Different Relative Humidities (RHs) for a Period

The bars of HTPS and TPS/MMT were stored in closed containers in the presence of different compounds, namely, a saturated K_2CO_3 solution, a saturated $CuCl_2$ solution (providing RHs of 44 and 68%, respectively) [20] at 20 °C.

The water contents of HTPS and TPS/MMT nanocomposites at different RHs were calculated on the base of mass of HTPS and TPS/MMT nanocomposites absorbing water. The data were averages of 3 specimens.

Mechanical Testing

Mechanical testing (National standard of China GB1040-79) of samples was determined in the AX M350-10KN Materials Testing Machine (Testometric, Rochdate, UK) at a crosshead speed of 50 mm/min. The data were averages of 5 specimens. The statistical significance was assessed by t-test (Solver in Origin 6.1 software).

Results and Discussions

Morphology

Scanning Electron Microscopy (SEM)

The morphology of MMT, starch and HTPS was shown in Fig. 2. MMT was micron-grade particles. Corn starch was granular. The HTPS could form the continuous phase. Due to the high shear and temperature conditions with the action of plasticizer, starch granules were molten or physically broken up into small fragments, HF penetrated into the starch granules and formed hydrogen bonds with

Fig. 2 SEM micrograph of **a** MMT, **b** corn starch, and **c** HTPS containing 30% HF
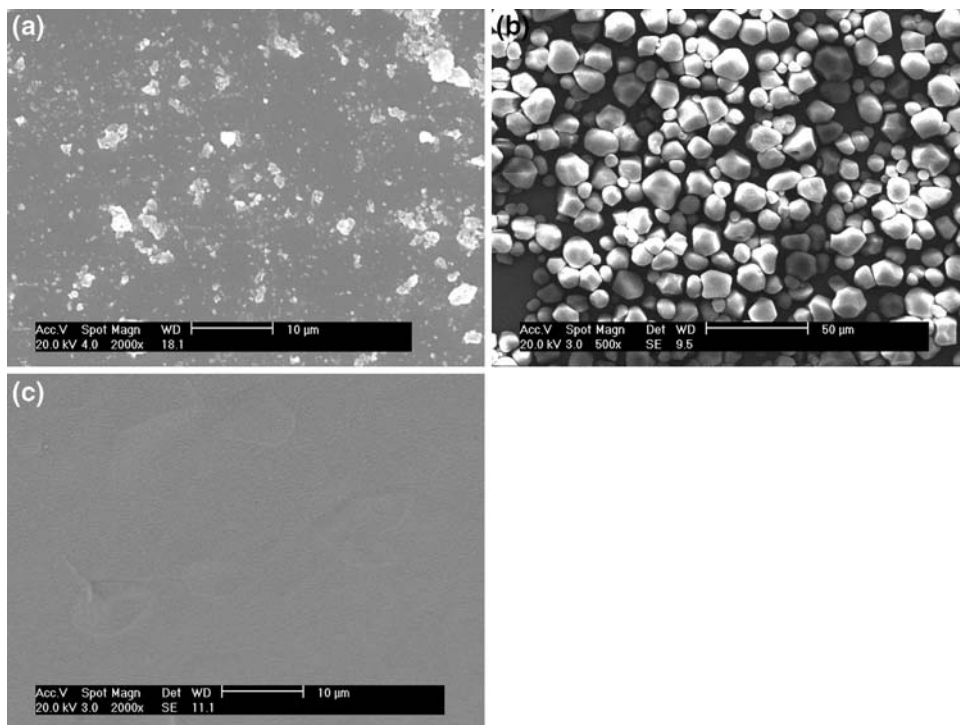
starch molecules, which weakened the strong action of starch intermolecular and intramolecular hydrogen bonds. The starch was plasticized by HF.

Atomic Force Microscopy (AFM)

AFM was used to examine nanoclay dispersion in TPS/MMT samples containing 2% MMT. The box in Fig. 3 indicated exfoliated MMT nanoclay. Well-dispersed and exfoliated nanocomposites platelets were shown in Fig. 3. The circle in Fig. 3 indicated micron-grade MMT particles. This indicated that the sample contained a combination of exfoliated MMT nanoclay and micron-grade MMT particles. The MMT was responsible for the evolution of the new nanophase separated morphology, where the layered silicates were embedded in the TPS as shown in the corresponding three-dimensional image in Fig. 3.
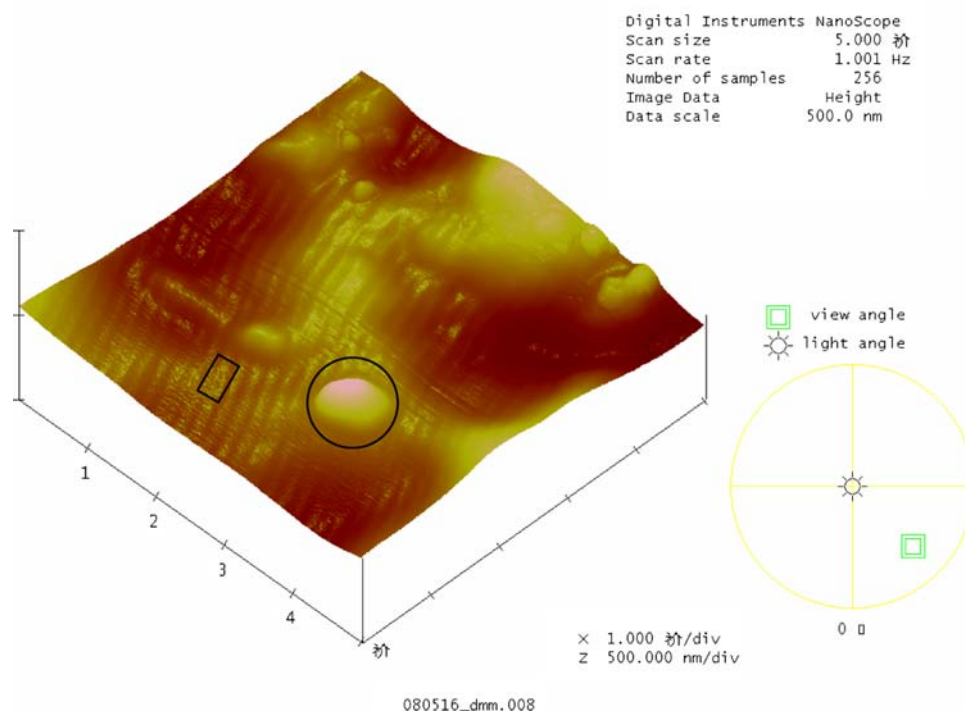
The sum of van der Walls force and electrostatic attractive force were against clay exfoliation, while the shearing force and thermal effect favored clay exfoliation. Clay exfoliation in polymer matrix by melt compounding mainly depended on one processes, namely, nanoclay layers exfoliation under shearing force and thermal effect. At the same time, swelling the MMT in HF resulted in the adsorption of some of the HF and extension of MMT distance. The extension of MMT distance could be proven by XRD. The extension of MMT favored the exfoliation of MMT.
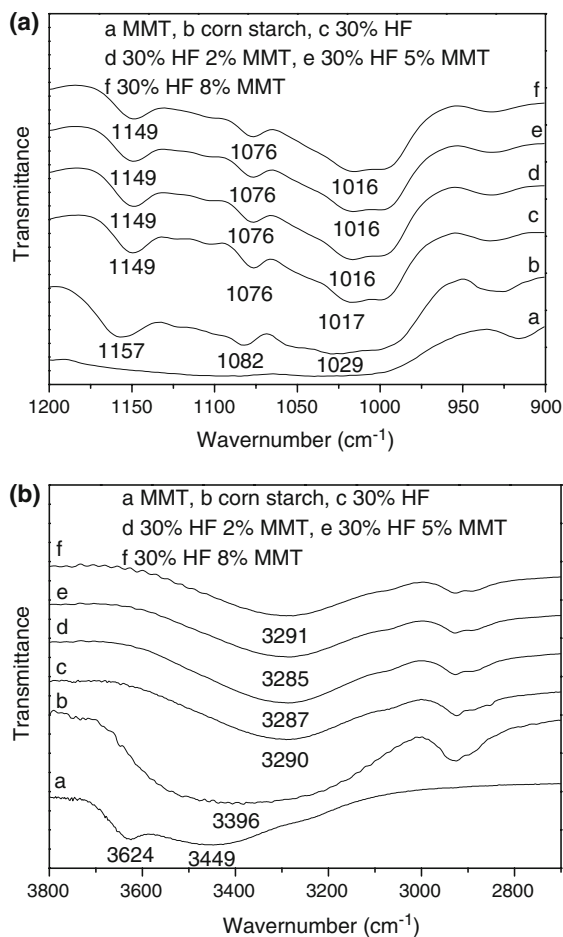
FT-IR Analysis

The wavenumber shift of stretching vibrations of corn starch could be observed in Fig. 4 (corn starch, HTPS and TPS/MMT). The peak wavenumber 1157 cm^{-1} was ascribed to the C–O bond stretching of the C–O–H group in starch. The characteristic peaks at 1082 and 1029 cm^{-1} were attributed to C–O bond stretching of the C–O–C group in the anhydroglucose ring of starch [21]. The peak wavenumber 3396 cm^{-1} was attributed to starch O–H bond stretching. In HTPS, all the peaks shifted to lower wavenumbers, for example, the peaks 1157 and 1082 cm^{-1} in starch shifted to 1149 and 1076 cm^{-1} in HTPS, respectively.

The analysis of FT-IR spectra of the blends enabled the hydrogen bond interactions to be identified [22]. Hydrogen bonds between plasticizer and starch were directly related to the wavenumber shift of the stretching bands of functional groups in starch. The lower the peak wavenumber was, the stronger the interaction was [23]. All these results indicated that stronger hydrogen bonds were formed between HF and starch compared with intra- and intermolecular hydrogen bonds in starch. FT-IR spectra had been analyzed, because of the groups –O–H and –CO–N in HF, stable hydrogen bonds were formed between HF and starch, which could weaken the intra- and intermolecular hydrogen bonds in starch, starch was plasticized.

Fig. 3 AFM micrograph of TPS/MMT containing 30% HF and 2% MMT

(a)
a MMT, b corn starch, c 30% HF
d 30% HF 2% MMT, e 30% HF 5% MMT
f 30% HF 8% MMT

(b)
a MMT, b corn starch, c 30% HF
d 30% HF 2% MMT, e 30% HF 5% MMT
f 30% HF 8% MMT

Fig. 4 a, **b** FT-IR spectra of MMT, corn starch, HTPS and TPS/MMT
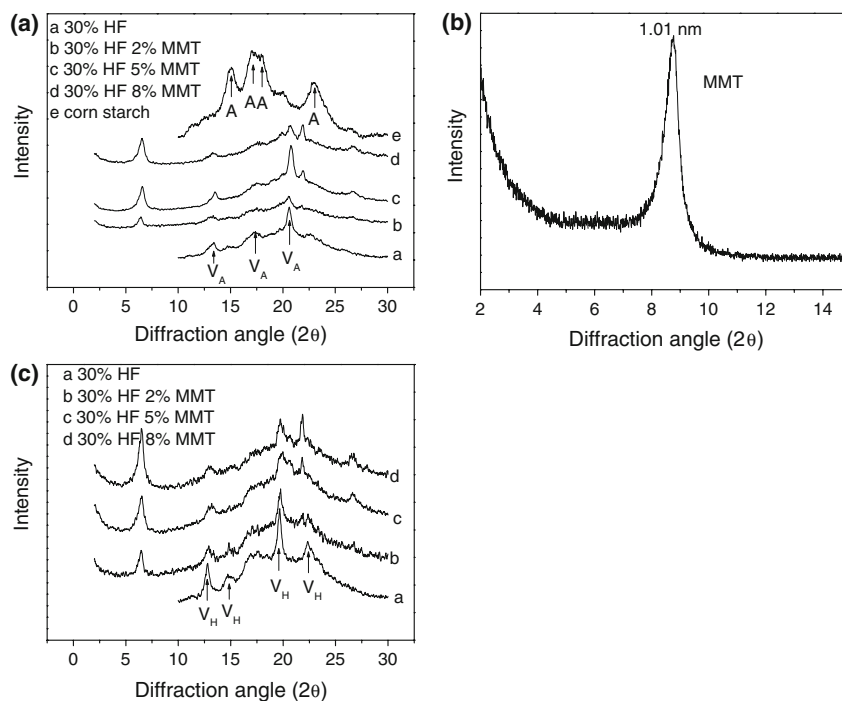
Figure 4 showed that the OH stretching peak, ascribed to the free hydroxyl groups, appeared at 3624 cm^{-1}, and the OH stretching peak, ascribed to the hydroxyl groups that participated in the formation of hydrogen bond, appeared at 3449 cm^{-1} in MMT [24]. In TPS/MMT, all the peaks above 3000 cm^{-1} shifted to lower wavenumbers, for example, the peaks 3624 and 3449 cm^{-1} in MMT shifted to around 3287 cm^{-1} in TPS/MMT. Compared with MMT, those peaks shifted to the lower wavenumbers. This indicated that in the preparation of TPS/MMT, in the presence of HF and the corporation of mechanical effect and thermal effect, new hydrogen bonds were formed among the hydroxyl groups in MMT molecules, HF and the hydroxyl groups in starch molecules. The hydrogen bonds made the OH stretch peak shifted to the lower wavenumber. The result of IR analysis indicated MMT, HF and starch had good compatibility, which was propitious to form the nanophase of MMT in the composites.

X-Ray Diffraction Analysis (XRD)

The X-ray diffraction patterns of corn starch, HTPS and TPS/MMT exposed to the air (the RH was around 50%) for 7 days were shown in Fig. 5a. The crystallinity of corn starch was ascribed to A-type (Fig. 5a, line e). V_A-type crystallinity were formed in HTPS (Fig. 5a, line a) [25]. During processing, as the plasticizer, HF molecules entered into starch particles, replaced starch intermolecular and intramolecular hydrogen bonds, and destroyed the crystallinity of starch. A-type crystallinity of corn starch

Fig. 5 a Diffractogram of corn starch, HTPS and TPS/MMT exposed to the air for 7 days, **b** diffractogram of MMT, and **c** diffractogram of HTPS and TPS/MMT exposed to the air for 90 days

(a)
a 30% HF
b 30% HF 2% MMT
c 30% HF 5% MMT
d 30% HF 8% MMT
e corn starch

(b) 1.01 nm MMT

(c)
a 30% HF
b 30% HF 2% MMT
c 30% HF 5% MMT
d 30% HF 8% MMT

disappeared and other crystallinity (V_A-type) were formed in HTPS. According to van Soest et al. [25], the V_A structure were preferably formed in materials containing relatively little water content, generally below 10% (w/w). Due to the low moisture content (7.62%) of starch, the V_A-type crystallinity was formed in HTPS [25].

MMT exhibited a sharp peak (001) at $2\theta = 8.76°$ (Fig. 5b) corresponding to the spacing of 1.01 nm (calculated by Bragg equation) between individual MMT layers, called d-spacing. The peak (001) was very sharp for all the TPS/MMT too. The d-spacing of MMT was 1.37 nm for TPS/MMT (Fig. 5a). It was not large enough for intercalation of starch. The expansion of MMT d-spacing was due to absorption of HF for MMT. In the opinion, the expansion of MMT d-spacing still favored exfoliation of MMT. It was presumed that the high shear and temperature conditions could destruct the layered structure of MMT in the presence of HF.

V_A-type crystallinity was formed in TPS/MMT (Fig. 5a, line c) too. According to Rappenecker and Zugenmaier [26] and Buléon et al. [27], V_H led to V_A upon dehydration, conversely V_A led to V_H upon hydration. After the samples HTPS and TPS/MMT were exposed to the air for 90 days, V_A type crystallinity was also changed to V_H due to hydration (Fig. 5c).

Thermogravimetric Analysis (TGA)

Compared with organic material, the inorganic materials had better thermal stability, due to its configuration characteristic. Therefore, the introduction of inorganic particles would greatly improve the thermal stability of organic polymer materials. As shown in Fig. 6, TGA was performed to examine the thermal stability of HTPS and TPS/MMT. The initial decomposition temperatures ($T_{d\ ini}$) were the temperatures at the 5% mass loss [11]. MMT improved
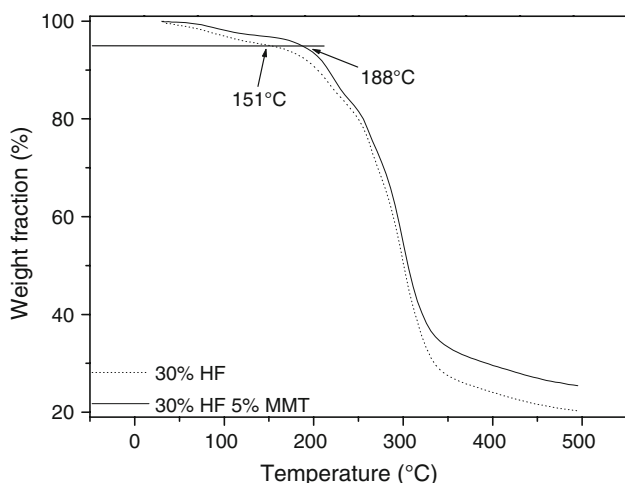
the initial decomposition temperature of HTPS. The TPS/MMT exhibited $T_{d\ ini}$ at 188 °C, which was higher than that of HTPS (151 °C). The TPS/MMT showed improved thermal stability compared to the HTPS sample, it could be attributed to the MMT acting as a barrier to the volatile products during heating.

Water Vapor Absorption

Water vapor absorption was an important index to estimate application of a composite. Figure 7 showed the water vapor absorption of HTPS and TPS/MMT at RH 44 and 68%. The water contents of TPS/MMT were less than that of HTPS. These indicated that the water resistance of nanocomposites was better than that of HTPS. The reason was that the maze structure was formed between the starch molecular chains and the MMT. If water molecules were absorbed into the materials, it had to go through this winding channel (maze structure), which reduced the
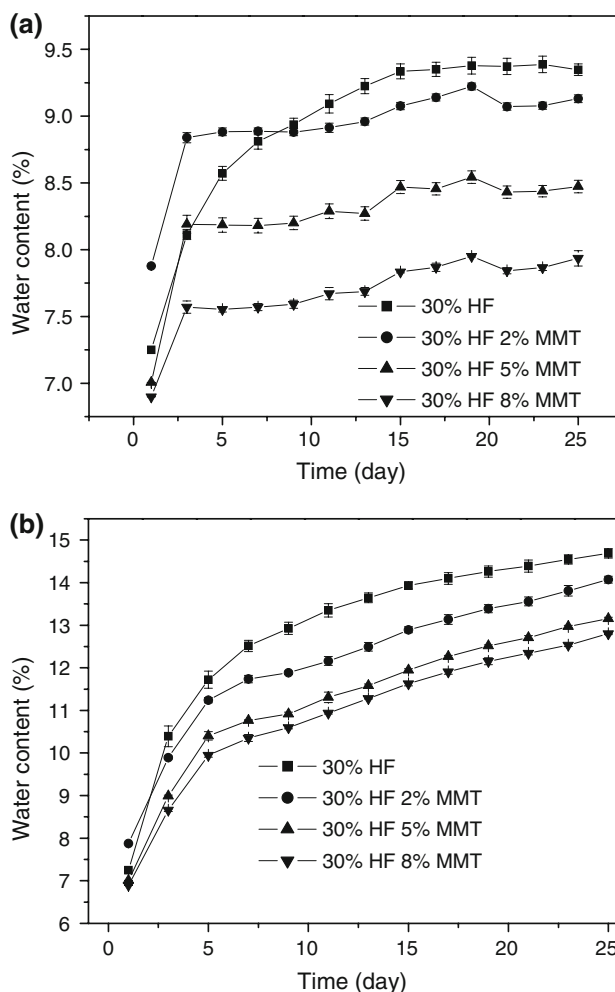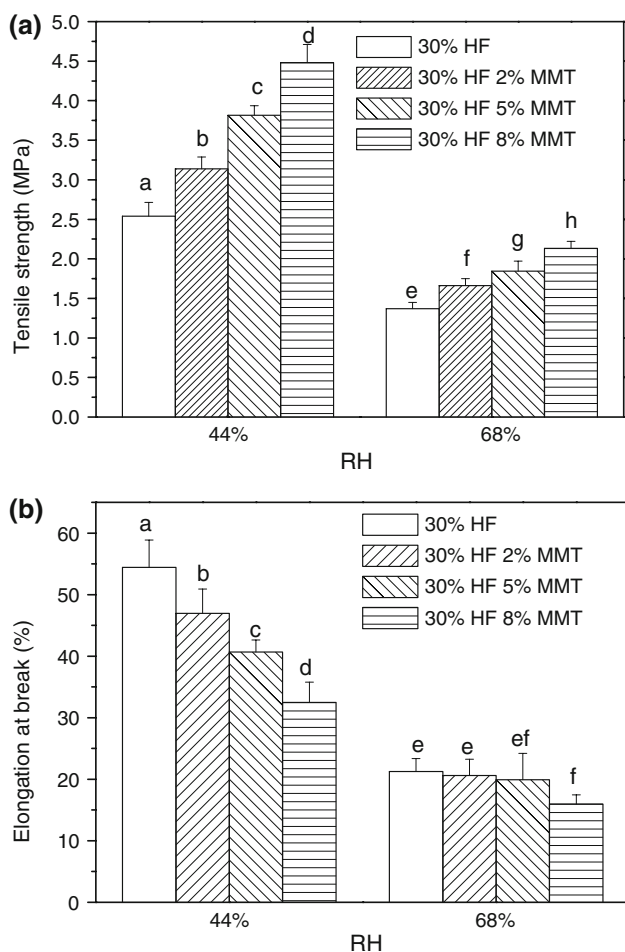

Fig. 7 Water contents of HTPS and TPS/MMT as function of storage time at **a** 44% and **b** 68% RH

Fig. 6 TGA curves of HTPS and TPS/MMT

Fig. 8 **a** Tensile strengths and **b** elongations at break of HTPS and TPS/MMT stored at different RHs for 28 days

diffusion speed of water molecules in the material, and so improved the water resistance.

Mechanical Properties

Figure 8 showed the tensile properties of HTPS and TPS/MMT nanocomposites with different MMT contents. It could be found that the tensile strength of TPS/MMT nanocomposites generally improved with increasing MMT content, but just the reverse for elongation at break. This increase of tensile strength was due to the exfoliated MMT, which increased the compatibility and dispersion between MMT and HTPS. MMT could effectively take effects of physical cross linking and reinforced the TPS matrix [28].

Conclusions

HF was synthesized by an efficient and practical method and proven to be effective as a novel plasticizer for corn

starch and a novel swelling agent for MMT. Stable hydrogen bonds among MMT, HF and starch were formed in TPS/MMT, as shown by the analysis of the FT-IR spectra. From the analysis of SEM, starch granules were completely disrupted and a continuous phase was obtained. Partial exfoliation TPS/MMT nanocomposites were formed as shown by the analysis of the AFM. X-ray diffraction analysis indicated A-type crystallinity of corn starch disappeared and starch was plasticized by HF, d-space of MMT in TPS/MMT was expanded. The TPS/MMT showed improved thermal stability compared to HTPS sample. TPS/MMT was material with better water resistance than HTPS. Generally, the tensile strengths of TPS/MMT were higher than those of HTPS, but just the reverse for elongations at break.

References

1. Ma XF, Yu JG (2004) J Appl Polym Sci 93:1769
2. Forssell PM, Mikkilä JM, Moates GK, Parker R (1997) Carbohydr Polym 34:275
3. Da Róz AL, Carvalho AJF, Gandini A, Curvelo AAS (2006) Carbohydr Polym 63:417
4. Tristao de Andrade C, Rocha de Souza RC (2004) BR Patent 2002000174
5. Wang L, Shogren RL, Carriere C (2000) Polym Eng Sci 40:499
6. Barrett A, Kaletunc G, Rosenburg S, Breslauer K (1995) Carbohydr Polym 26:261
7. Stein TM, Greene RV (1997) Starch/Stärke 49:245
8. Yang JH, Yu JG, Ma XF (2006) Starch/Stärke 58:330
9. Wang N, Yu JG, Chang PR, Ma XF (2008) Carbohydr Polym 71:109
10. Park HM, Lee WK, Park CY, Cho WJ, Ha CS (2003) J Mater Sci 38:909
11. Zhang QX, Yu ZZ, Xie XL, Naito K, Kagawa Y (2007) Polymer 48:7193
12. Ishida H, Campbell S, Blackwell J (2000) Chem Mater 12:1260
13. Li Y, Ishida H (2003) Polymer 44:6571
14. Bagdi K, Muller P, Pukanszky B (2006) Compos Interface 13:1
15. Tarvainen M, Sutinen R, Somppi M, Paronen P, Poso A (2001) Pharm Res 18:1760
16. Coupland K, Smith PJ (1986) Spec Chem 6:10
17. Kibler WR (1973) US Patent 3760578
18. Ricci A, Sbrana G, Braca G (1991) EP Patent 0248259
19. Frings RB, Grahe GF (1992) EP Patent 469550
20. Godbillot L, Dole P, Joly C, Rogé B, Mathlouthi M (2006) Food Chem 96:380
21. Fang JM, Fowler PA, Tomkinson J, Hill CAS (2002) Carbohydr Polym 47:245
22. Aoi K, Takasu A, Tsuchiya M, Okada M (1998) Macromol Chem Phys 199:2805
23. Pawlak A, Mucha M (2003) Thermochim Acta 396:153
24. Huang MF, Yu JG, Ma XF (2004) Polymer 45:7017
25. van Soest JJG, Hulleman SHD, de Wit D, Vliegenthart JFG (1996) Ind Crop Prod 5:11
26. Rappenecker G, Zugenmaier P (1981) Carbohydr Res 89:11
27. Buléon A, Delage MM, Brisson J, Chanzy H (1990) Int J Biol Macromol 12:25
28. Ma XF, Yu JG, Wang N (2007) Macromol Mater Eng 292:723